J. Fluid Mech. (1985), *vol.* 153, *pp.* 417–439
Printed in Great Britain

Boundary effects on electrophoretic motion of colloidal spheres

By H. J. KEH† AND J. L. ANDERSON

Department of Chemical Engineering, Carnegie-Mellon University, Pittsburgh, PA 15213

(Received 25 July 1984 and in revised form 13 November 1984)

An analysis is presented for electrophoretic motion of a charged non-conducting sphere in the proximity of rigid boundaries. An important assumption is that $\kappa a \rightarrow \infty$, where a is the particle radius and κ is the Debye screening parameter. Three boundary configurations are considered: single flat wall, two parallel walls (slit), and a long circular tube. The boundary is assumed a perfect electrical insulator except when the applied field is directed perpendicular to a single wall, in which case the wall is assumed to have a uniform potential (perfect conductor). There are three basic effects causing the particle velocity to deviate from the value given by Smoluchowski's classic equation: first, a charge on the boundary causes electro-osmotic flow of the suspending fluid; secondly, the boundary alters the interaction between the particle and applied electric field; and, thirdly, the boundary enhances viscous retardation of the particle as it tries to move in response to the applied field. Using a method of reflections, we determine the particle velocity for a constant applied field in increasing powers of λ up to $O(\lambda^6)$, where λ is the ratio of particle radius to distance from the boundary. Ignoring the $O(\lambda^0)$ electro-osmotic effect, the first effect attributable to proximity of the boundary is $O(\lambda^3)$ for all boundary configurations, and in cases when the applied field is parallel to the boundaries the electrophoretic velocity is proportional to $\zeta_p - \zeta_w$, the difference in zeta potential between the particle and boundary.

1. Introduction

The electrophoretic velocity of a single colloidal particle suspended in a fluid of viscosity η and dielectric constant ϵ is related to the applied electric field by Smoluchowski's formula:

$$U_0 = \left(\frac{\epsilon \zeta_p}{4\pi\eta}\right) E_\infty, \tag{1.1}$$

where ζ_p is the 'zeta potential' of the particle surface, which is normally taken to be the electrostatic potential at the inner edge of the diffuse part of the electrical double layer surrounding the particle (Adamson 1982; Hunter 1981). The ratio U_0/E_∞ is defined to be the electrophoretic mobility, and equals the term in parentheses, the magnitude of which is typically of order (μm/s)/(V/cm). The Smoluchowski equation applies to particles of any shape (Morrison 1970), and there is no rotation of the particle.

Several assumptions were made to derive (1.1), and the subscript 0 on U_0 is used to emphasize the existence of these assumptions. First, ζ_p must be uniform over the

† Present address: Department of Chemical Engineering, National Taiwan University, Taipei 107 Taiwan, R.O.C.

surface of the particle, at least over distances comparable to the particle dimension. 'Discrete-charge' effects, reflecting the existence of heterogeneity in surface charge on lengthscales $O(\kappa^{-1})$, where κ^{-1} is the Debye screening length, do not seem to be important, except that they might slightly alter the value of ζ_p from that predicted by the classical Gouy–Chapman theory of the diffuse double layer (Levine, Mingins & Bell 1967). Another assumption is referred to as the 'thin-double-layer approximation', or 'Helmholtz limit', and requires that κ^{-1} be infinitesimal relative to particle dimensions; for a sphere this would mean $\kappa a \rightarrow \infty$ where a equals the sphere radius. In the derivation of (1.1), a constant applied field has always been assumed; however, in §3 of this paper we show that this assumption is unnecessary and (1.1) holds even if $\boldsymbol{E}_\infty$ varies over distances comparable to the particle size. The fourth assumption is that the particle is suspended in an infinite fluid, meaning that boundaries are sufficiently far removed from the particle so that they have negligible effect on the electric and fluid velocity fields associated with the particle. In this paper, we relax this assumption and examine how certain rigid boundaries affect electrophoretic motion.

Most attention in the literature has been paid to the thin-double-layer approximation, and several monographs (e.g. Dukhin & Derjaguin 1974; Hunter 1981) review progress in this area. In the past several years important advances have been made in developing analytical expressions to correct (1.1) for finite κa of spherical particles (e.g. O'Brien & Hunter 1981), and extensive numerical results are available for a wide range of κa and ζ_p (O'Brien & White 1978). These show that the thin-double-layer approximation is accurate when

$$(\kappa a)^{-1} \cosh (Ze\zeta_p/2kT) \ll 1, \tag{1.2}$$

where Z is the charge number of the electrolyte, assumed the same for both ions, and e is the charge of one proton.

In the application of electrophoresis to particle analysis or separation, natural convection of the suspending fluid due to ohmic heating and non-uniform heat transfer creates problems. To avoid such mixing, porous media are often used to contain the suspension. Porous membranes could even be used to achieve high electric fields and separation of particles by both size and charge. Other examples of bounded systems include electrophoresis of small particles through porous rock, through coatings formed by larger particles, and through a Coulter counter designed not only to count and size the particles but also to determine their zeta potentials (DeBlois & Bean 1970). In all such systems one must question the applicability of (1.1) and determine if the boundaries significantly affect movement of the particles.

Here we model the electrophoretic motion of spherical, uniformly charged particles near rigid boundaries of different configurations. In all cases the thin-double-layer limit ($\kappa a \rightarrow \infty$) is taken. Only single particles are considered, and hence the results are limited to dilute suspensions. The applied electric field is assumed constant over distances comparable to the particle radius. The proximity of rigid boundaries leads to two effects. First, the interaction between particle and electric field is altered by the boundary, an effect that tends to enhance the electrophoretic velocity. Secondly, the fluid dynamics are affected in a way that tends to slow the particle. The second effect is stronger in the cases we have studied, and hence the net effect is a retardation of the particle's velocity.

In §2 the governing equations for mass and charge transport, fluid flow and electrostatics are organized and simplified through scaling arguments in two defined regions, 'inner' and 'outer', where the former is the fluid contained within distances

$O(\kappa^{-1})$ from the particle surface and from the boundaries. Because large κa is assumed, the equations of the inner region can be integrated directly to provide surface conditions for the outer region, consistent with the analysis of O' Brien (1983). Section 3 contains a brief derivation that shows that (1.1) applies to unbounded systems in which the undisturbed field $\boldsymbol{E}_{\infty}$ varies appreciably over distances comparable to a, with $\boldsymbol{E}_{\infty}$ evaluated at the position of the particle's centre. This result is used, along with Faxen's law for the velocity of a force-free sphere suspended in an arbitrary velocity field, to reflect the electric and velocity fields between particle and boundary. The correction for the boundary is presented in a power series in λ:

$$\boldsymbol{U} = \left[\sum_{m=0}^{\infty} b_m \lambda^m\right] \boldsymbol{E}_{\infty}, \tag{1.3}$$

where λ equals the ratio of particle radius to the distance of the particle centre from the boundary. The first effect of finite λ is $O(\lambda^3)$, rather than $O(\lambda)$ as for problems involving sedimentation (Happel & Brenner 1973), so boundary effects on electrophoresis are relatively weak. In situations where the boundary is non-conducting and $\boldsymbol{E}_{\infty}$ is directed parallel to it, the coefficients b_m are proportional to $\zeta_p - \zeta_w$, the difference in zeta potentials between particle and boundary. The wall potential enters in these cases because the applied field interacts with the double layer at the boundary to produce an electro-osmotic flow. Section 4 is concerned with a single flat wall, while movement of a particle along the axis of a long slit or circular pore is considered in §5. The main results are given in (4.16), (4.26), (5.9) and (5.19), which apply to *open* systems where no pressure gradients are established to control the overall volumetric flow (as discussed in §6).

2. Governing equations for thin double layers

By 'thin' double layers we mean situations where transport processes outside the double layer have negligible effect on the ion distributions within the double layer, and hence these distributions are determined by the equilibrium structure of the double layer. The criterion for this is given by (1.2). Furthermore, we wish to model the fluid/solid interface as an infinite flat surface on lengthscales of κ^{-1}. If the smallest principal radius of curvature of the interface is a^* then the flat-plate model has an error $O(\kappa a^*)^{-1}$; therefore letting $\kappa a^* \to \infty$ allows the flat-surface approximation.

The fluid phase is divided into two regions: (1) an 'inner' region defined as the double layer adjacent to the particle and the solid boundaries, where the important lengthscale is the Debye length κ^{-1}; and (2) an 'outer' region defined as the remainder of the fluid, where the particle dimension is the approximate lengthscale (see figure 1). Because the space charge density ρ_e approaches zero as $\exp(-\kappa\hat{y})$, where $\hat{y}$ is the distance from an interface, the outer region is electrically neutral ($\rho_e = 0$). The steady-state electrostatic and transport equations applicable to both regions are the following:

$$\nabla^2 \Phi = -\frac{4\pi}{\epsilon} \rho_e, \tag{2.1}$$

$$\eta \nabla^2 \boldsymbol{v} - \nabla p - \rho_e \nabla \Phi = \boldsymbol{0}, \tag{2.2}$$

$$\nabla \cdot \boldsymbol{v} = 0, \tag{2.3}$$

$$\nabla \cdot \boldsymbol{N}_i = 0, \tag{2.4}$$

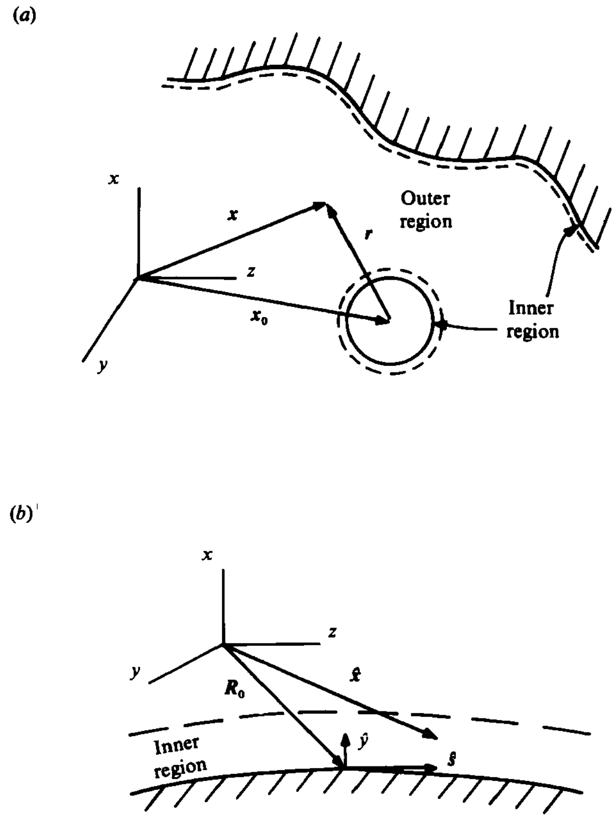

FIGURE 1. (*a*) Sketch of inner and outer regions of the fluid phase for a colloidal sphere near a solid boundary. (*b*) Geometry of the inner region (the double layer adjacent to the fluid/solid interface, with a thickness $O(\kappa^{-1})$).

$$\nabla\cdot\sum_i Z_i e\boldsymbol{N}_i = 0, \tag{2.5}$$

$$\boldsymbol{N}_i = -D_i\left[\nabla C_i + \frac{Z_i e C_i}{kT}\nabla\Phi\right] + C_i\boldsymbol{v}, \tag{2.6}$$

$$\rho_e = \sum_i Z_i e C_i. \tag{2.7}$$

Equation (2.1) is the Poisson equation, while (2.2)–(2.3) are the Stokes equations. Equation (2.6) is the Nernst–Planck equation for the flux $\boldsymbol{N}_i$ of ionic species i having charge $Z_i e$ per ion, where e is the charge of one proton, and diffusion coefficient D_i. There is some question as to the accuracy of the Nernst–Planck equation at moderate-to-high ion concentrations (say $\gtrsim 10^{-1}$ g mol/litre), but it is really needed here only to provide scaling arguments to allow solution of (2.2) inside the double layer. Φ is the electrical potential relative to the potential the fluid would have at the position $\boldsymbol{x}_0$ of the particle if the particle were not there. Equation (2.5) is redundant with (2.4), but is useful in the outer region ($\rho_e = 0$) to decouple $\boldsymbol{v}$ from the calculation of $\Phi(\boldsymbol{x})$, since (2.1) cannot be used there (Newman 1973).

The boundary conditions at the fluid/solid interfaces of the particle and the boundaries are the following:

$$\boldsymbol{n}\cdot\boldsymbol{N}_i = \boldsymbol{n}\cdot\boldsymbol{v}^* C_i, \quad \boldsymbol{v} = \boldsymbol{v}^*, \quad \boldsymbol{n}\cdot\nabla\Phi = -\frac{4\pi}{\epsilon}\sigma. \tag{2.8a, b, c}$$

$\boldsymbol{n}$ is the unit normal pointing into the fluid phase. Equation (2.8*a*) means no charge can be conducted across the surface, consistent with our assumption that the solid phases are non-conducting. $\boldsymbol{v}^*$ is the velocity of the interface, equal to zero for the fixed solid boundaries and $\boldsymbol{U}+\boldsymbol{\Omega}\times\boldsymbol{r}$ for a particle translating at velocity $\boldsymbol{U}$ and rotating at angular velocity $\boldsymbol{\Omega}$. Equation (2.8*c*) is the Gauss condition at the 'slip plane' of the double layer, with σ equal to the charge density. σ is assumed constant on the interfaces, but could differ in sign and magnitude between particle and boundary. Possible Stern-layer effects are not considered in this analysis. Far from the particle in the outer region the conditions are

$$C_i \rightarrow C_{i\infty} = \text{constant}, \quad \Phi \rightarrow \Phi_\infty(\boldsymbol{x}), \tag{2.9a, b}$$

where Φ_∞ satisfies Laplace's equation.

Inner region

Variables in this region are denoted by a hat ($\hat{}$) over them. Let $\boldsymbol{R}_0$ be a position on the fluid/solid interface, either on the particle or boundary, and $\hat{\boldsymbol{x}}$ be a position within the fluid portion of the double layer adjacent to the interface. A local coordinate system is defined by (see figure 1*b*)

$$\hat{\boldsymbol{x}} - \boldsymbol{R}_0 = \hat{y}\boldsymbol{n} + \hat{\boldsymbol{s}}, \tag{2.10}$$

such that the fluid/solid interface is described by $\hat{y} = 0$ with an error $O(\kappa a^*)^{-1}$. $\boldsymbol{n}$ is the unit normal at $\boldsymbol{R}_0$, and $\hat{\boldsymbol{s}}$ is the two-dimensional position vector from $\boldsymbol{R}_0$ in the tangent plane. The scale of $\hat{y}$ is κ^{-1}. By examining (2.1)–(2.7) we find the following characteristic values:

$$\frac{\partial \hat{\Phi}}{\partial \hat{y}} \approx \kappa \frac{kT}{e} \quad \left(\text{since } |\zeta| \approx \frac{kT}{e}\right), \tag{2.11a}$$

$$\left|\frac{\partial \hat{\Phi}}{\partial \hat{\boldsymbol{s}}}\right| \approx E_\infty, \tag{2.11b}$$

$$|\hat{\boldsymbol{v}}| \approx \frac{\epsilon kT}{4\pi\eta e} E_\infty, \tag{2.11c}$$

$$\frac{\partial \hat{v}_y}{\partial \hat{y}} \sim \frac{|\hat{\boldsymbol{v}}|}{a^*}. \tag{2.11d}$$

E_∞ is the magnitude of the applied electrical field ($E_\infty = |\nabla \Phi_\infty|$). In the limit $\kappa a \rightarrow \infty$ (2.1) and (2.4)–(2.7) can be used with the above characteristic values and boundary condition (2.8*a*) to show that

$$\hat{\Phi} = \hat{\psi}(\hat{y}) + \hat{\Phi}_\mathrm{b}(\hat{\boldsymbol{s}}), \tag{2.12}$$

where $\hat{\psi}$ is attributable to the interfacial charge σ and is independent of $\hat{\boldsymbol{s}}$ as long as the C_i are constant in the outer region (as they are). $\hat{\psi}$ is $O(kT/e)$ and decays to zero as $\exp(-\kappa\hat{y})$, while $\hat{\Phi}_\mathrm{b}$ must match with the electrical potential determined from the equations of the outer region.

Combining (2.12) with (2.1) and (2.2) and using the characteristic values in (2.11), the following is obtained when $\kappa a \rightarrow \infty$:

$$\eta \frac{\partial^2 \hat{\boldsymbol{v}}^{(s)}}{\partial \hat{y}^2} + \left(\frac{\epsilon}{4\pi}\frac{\mathrm{d}^2 \hat{\psi}}{\mathrm{d}\hat{y}^2}\right)\frac{\partial \hat{\Phi}_\mathrm{b}}{\partial \hat{\boldsymbol{s}}} = \boldsymbol{0}, \tag{2.13}$$

where $\hat{\boldsymbol{v}}^{(s)} = (\boldsymbol{I}-\boldsymbol{nn})\cdot\hat{\boldsymbol{v}}$ and $\boldsymbol{I}$ is the unit dyadic. Integrating twice over $\hat{y}$, with 'no slip' at the fluid/solid interface ($\hat{y} = 0$), gives

$$\hat{\boldsymbol{v}}^{(s)} = \frac{\epsilon}{4\pi\eta}(\zeta - \hat{\psi}(\hat{y}))\frac{\partial \boldsymbol{\Phi}_{\mathrm{b}}}{\partial \hat{\boldsymbol{s}}} + (\boldsymbol{I}-\boldsymbol{nn})\cdot\boldsymbol{v}^*, \tag{2.14}$$

where ζ is the zeta potential, defined as $\hat{\psi}(0)$. The first term on the right-hand side of (2.14) is the well-known Helmholtz expression for electro-osmotic flow induced by an electric field tangent to a solid surface. To $O((\kappa a)^0)$ the normal component of fluid velocity is $\hat{v}_n = \boldsymbol{n}\cdot\boldsymbol{v}^*$. Combining the normal and tangential components and letting $\hat{y}\rightarrow\infty$, we have fluid velocity at the outer edge of the double layer:

$$\boldsymbol{v}_s \equiv \lim_{\kappa\hat{y}\rightarrow\infty}(\hat{\boldsymbol{v}}) = \boldsymbol{v}^* - \frac{\epsilon\zeta}{4\pi\eta}\boldsymbol{E}_s, \tag{2.15}$$

where it is understood that $\boldsymbol{E}_s = -\partial\hat{\Phi}_{\mathrm{b}}/\partial\hat{\boldsymbol{s}}$ and is perpendicular to $\boldsymbol{n}$. The interfacial velocity of the particle is

$$\boldsymbol{v}^* = \boldsymbol{U} + \boldsymbol{\Omega}\times\boldsymbol{r},$$

where $\boldsymbol{U}$ is the velocity of the reference point $\boldsymbol{x}_0$ in the particle, $\boldsymbol{\Omega}$ is the angular velocity and $\boldsymbol{r} = \boldsymbol{x}-\boldsymbol{x}_0$ evaluated on the solid/fluid interface. $\boldsymbol{v}^*$ equals zero for the fixed boundaries.

Outer region

The appropriate lengthscale is a^*. Since the ion concentrations are uniform far from the particle and outside the double layer of the boundary, and ρ_e is essentially zero in the entire outer region, (2.4)–(2.6) can be used to show that all C_i are constant in the outer region. Equation (2.5) thus reduces to

$$\nabla^2\Phi = 0, \tag{2.16}$$

with boundary condition (2.9*b*). Let $\boldsymbol{R}$ represent the surfaces of the particle and boundary as approached from the outer region. The behaviour of Φ in the vicinity of $\boldsymbol{R}$ must be consistent with $\hat{\Phi}$ in the limit $y\rightarrow\infty$. From (2.12) we see that the appropriate condition on the surfaces of the outer region is

$$\boldsymbol{n}\cdot\nabla\Phi = 0 \quad \text{on } \boldsymbol{R}. \tag{2.17}$$

This condition says that no current can be conducted into the double layer, because it is so thin relative to a^*. Solving (2.16) with (2.9*b*) and (2.17) and evaluating Φ at $\boldsymbol{x}\rightarrow\boldsymbol{R}$ gives the value of $\boldsymbol{E}_s$ to be used in (2.15):

$$\boldsymbol{E}_s = \lim_{\boldsymbol{x}\rightarrow\boldsymbol{R}}(-\nabla\Phi). \tag{2.18}$$

Given the surface velocity $\boldsymbol{v}_s$, as calculated from (2.15) and (2.18) on all points $\boldsymbol{R}$ on the surfaces of the particle and boundary, the velocity field can be determined from the Stokes equations:

$$\eta\nabla^2\boldsymbol{v} - \nabla p = \boldsymbol{0}, \quad \nabla\cdot\boldsymbol{v} = 0, \tag{2.19a,b}$$

$$\boldsymbol{v} = \boldsymbol{U} + \boldsymbol{\Omega}\times\boldsymbol{r} + \frac{\epsilon\zeta}{4\pi\eta}(\boldsymbol{I}-\boldsymbol{nn})\cdot\nabla\Phi \quad \text{on the particle surface,} \tag{2.20a}$$

$$\boldsymbol{v} = \frac{\epsilon\zeta}{4\pi\eta}(\boldsymbol{I}-\boldsymbol{nn})\cdot\nabla\Phi \quad \text{on the boundary surface,} \tag{2.20b}$$

where we understand the term 'surface' to mean outer limit of the double layer. Because the particle surface encloses a *neutral* body (i.e. charged interface plus oppositely charged, diffuse space charge) and the particle is freely suspended in the fluid, the electric field produces no force or couple on the particle. Thus the force and couple by the fluid on the particle surface must be zero:

$$\boldsymbol{F}_{\mathrm{f}} = \iint_{\text{particle surface}} \boldsymbol{n}\cdot\boldsymbol{\tau}\,\mathrm{d}\mathscr{S} = \mathbf{0}, \quad \boldsymbol{T}_{\mathrm{f}} = \iint_{\text{particle surface}} \boldsymbol{r}\times(\boldsymbol{n}\cdot\boldsymbol{\tau})\,\mathrm{d}\mathscr{S} = \mathbf{0}, \qquad (2.21\,a,b)$$

where $\boldsymbol{\tau}$ is the stress dyadic. By satisfying (2.21), $\boldsymbol{U}$ and $\boldsymbol{\Omega}$ are determined. Maxwellian (electrical) terms are omitted from $\boldsymbol{\tau}$ because in this problem they would contribute only at $O(E^2_\infty)$, while we consider only linear phenomena.

Because the solid phases of the particle and boundary are assumed non-conducting in all but one derivation, there is no need to model the electrostatics of these phases. This assumption leads to boundary condition (2.17) for the electric field in the outer region. In the one exception (see §4), in which a particle moves normal to an infinite plane wall, the boundary is assumed to be a perfect conductor (i.e. an electrode), so that (2.17) is replaced in this case by the following:

$$\left.\begin{aligned} \Phi &= \text{constant} \quad \text{on the boundary surface,} \\ \boldsymbol{n}\cdot\nabla\Phi &= 0 \quad \text{on the particle surface.} \end{aligned}\right\} \qquad (2.22)$$

The reason for this change is that it is not realistic to have a constant undisturbed field $-\nabla\Phi_\infty$ directed normal to a plane wall and simultaneously satisfy (2.17).

In summary, matched expansions for electrical potential and fluid velocity have been constructed in the limit $\kappa a^* \to \infty$, where a^* is the principal radius of curvature of the interface between solid and fluid. The inner region produces condition (2.17) or (2.22) for Φ in the outer region and conditions (2.20) for $\boldsymbol{v}$. The strategy is to solve (2.16) for $\Phi(\boldsymbol{x})$, using (2.17) and (2.9*b*), then solve (2.19) and (2.20), and finally satisfy (2.21) to obtain $\boldsymbol{U}$ and $\boldsymbol{\Omega}$. A 'method of reflections' (Happel & Byrne 1954) will be used to account for interactions between the particle and the boundary.

3. Fluid dynamics for a sphere in an arbitrary electric field

A non-conducting sphere of radius a and uniform zeta potential ζ_{p} is instantaneously positioned at $\boldsymbol{x}_0$ in an *unbounded* fluid. The relative position vector $\boldsymbol{r}$ is defined as $\boldsymbol{x}-\boldsymbol{x}_0$. The thin-double-layer assumption ($\kappa a \to \infty$) is applied. In the absence of the sphere, the electrical potential is $V_{\mathrm{A}}(\boldsymbol{x})$† such that $|a^2\nabla\nabla V_{\mathrm{A}}|$ could be comparable to $|a\nabla V_{\mathrm{A}}|$. To find the translational and angular velocities of the sphere, as well as the resulting velocity field in the fluid, we must solve Laplace's equation for $V(\boldsymbol{r})$ and the Stokes equations for $\boldsymbol{v}(\boldsymbol{r})$ in the outer region, $r-a \gg \kappa^{-1}$, as indicated in §2.

The electrical disturbance caused by the sphere, $V^* \equiv V - V_{\mathrm{A}}$, is governed by

$$\nabla^2 V^* = 0, \qquad (3.1)$$

$$\boldsymbol{n}\cdot\nabla V^* = -\boldsymbol{n}\cdot\nabla V_{\mathrm{A}} \quad (r = a^+), \qquad (3.2a)$$

$$V^* \to 0 \quad (r \to \infty), \qquad (3.2b)$$

where $\boldsymbol{n}$ is the unit normal, and $r = a^+$ designates the outer edge of the double layer.

† In this section we use V for the potential instead of Φ.

Note that $V_A(\boldsymbol{x})$ is assumed to satisfy Laplace's equation as well. A general solution to (3.1) that satisfies the second boundary condition is

$$V^* = \sum_{m=1}^{\infty} \boldsymbol{B}_m[\cdot]\boldsymbol{S}_m r^{-(m+1)}, \tag{3.3}$$

where the $\boldsymbol{S}_m$ are surface harmonics, which are mth-order polyadics defined by

$$\boldsymbol{S}_m = r^{m+1}\nabla^m(r^{-1}), \tag{3.4}$$

and the symbol $[\cdot]$ represents m scalar products. If the brackets $\langle f\rangle$ denote an average of f over the surface of a sphere,

$$\langle f\rangle \equiv \frac{1}{4\pi a^2}\iint_{r=a} f\,\mathrm{d}\mathscr{S}, \tag{3.5}$$

it can be shown that the $\boldsymbol{S}_m$ are orthogonal when such an average is taken:

$$\langle \boldsymbol{S}_m \boldsymbol{S}_n\rangle = 0 \quad \text{if } m \neq n.$$

The polyadic coefficients $\boldsymbol{B}_m$ are determined by expanding the right-hand side of (3.2a) about $r=0$ and comparing with (3.3). The first few terms are

$$\boldsymbol{B}_1 = -\tfrac{1}{2}a^3(\nabla V_A)_0, \quad \boldsymbol{B}_2 = \tfrac{1}{9}a^5(\nabla\nabla V_A)_0, \quad \boldsymbol{B}_3 = -\tfrac{1}{120}a^7(\nabla\nabla\nabla V_A)_0, \tag{3.6a,b,c}$$

where the subscript 0 denotes evaluation at $\boldsymbol{x} = \boldsymbol{x}_0$. Using these results and realizing that V_A satisfies Laplace's equation, we have

$$V^* = \frac{1}{2}\left(\frac{a}{r}\right)^3 \boldsymbol{r}\cdot(\nabla V_A)_0 + \frac{1}{3}\left(\frac{a}{r}\right)^5 \boldsymbol{rr}:(\nabla\nabla V_A)_0 + \frac{1}{8}\left(\frac{a}{r}\right)^7 \boldsymbol{rrr}\,\vdots\,(\nabla\nabla\nabla V_A)_0 + \dots \tag{3.7}$$

The disturbance to the electric field is obtained by taking the gradient of (3.7):

$$\boldsymbol{E}^* = \frac{1}{2}\left(\frac{a}{r}\right)^3\left[\boldsymbol{I} - 3\frac{\boldsymbol{rr}}{r^2}\right]\cdot(\boldsymbol{E}_A)_0 + \frac{1}{3}\left(\frac{a}{r}\right)^5\left[2\boldsymbol{Ir} - 5\frac{\boldsymbol{rrr}}{r^2}\right]:(\nabla\boldsymbol{E}_A)_0 + O(\nabla\nabla\boldsymbol{E}_A). \tag{3.8}$$

Note that the disturbance to the field is weak, decaying as r^{-3}. The electric field at the particle surface ($\boldsymbol{E}_s$), including both the original field plus the disturbance, is

$$\boldsymbol{E}_s = [\tfrac{3}{2}(\boldsymbol{E}_A)_0 + \tfrac{5}{3}a\boldsymbol{n}\cdot(\nabla\boldsymbol{E}_A)_0 + O(a^2\,\nabla\nabla\boldsymbol{E}_A)_0]\cdot[\boldsymbol{I} - \boldsymbol{nn}]. \tag{3.9}$$

Because the particle is assumed to be non-conducting, this field is directed in the plane of the surface and has no normal component.

In order to obtain the particle velocity and the fluid velocity field, we employ Lamb's general solution as outlined by Brenner (1964a). If $\boldsymbol{U}$ and $\boldsymbol{\Omega}$ are the translational and angular velocities of the particle, we can express the fluid velocity at the particle's surface (or, more precisely, at the outer edge of the double layer) using the solution for flow in the double layer that was developed in §2:

$$\boldsymbol{v}_s = \lim_{r\to a^+}(\boldsymbol{v}) = \boldsymbol{U} + a\boldsymbol{\Omega}\times\boldsymbol{n} - \frac{\epsilon\zeta_p}{4\pi\eta}\boldsymbol{E}_s. \tag{3.10}$$

The velocity and pressure fields for $r > a$ are completely specified when the coefficients $\boldsymbol{\alpha}_m$, $\boldsymbol{\beta}_m$, $\boldsymbol{\gamma}_m$ are determined at $r = a^+$ using the following:

$$\boldsymbol{n}\cdot\boldsymbol{v}_s = \sum_{m=1}^{\infty}\boldsymbol{\alpha}_m[\cdot]\boldsymbol{S}_m, \tag{3.11a}$$

$$-a\nabla\cdot\boldsymbol{v}_s = \sum_{m=1}^{\infty}\boldsymbol{\beta}_m[\cdot]\boldsymbol{S}_m, \tag{3.11b}$$

$$a\boldsymbol{n}\cdot(\nabla\times\boldsymbol{v}_s) = \sum_{m=1}^{\infty}\boldsymbol{\gamma}_m[\cdot]\boldsymbol{S}_m. \tag{3.11c}$$

The force and torque applied by the fluid on the surface $r = a^+$ are given by

$$\boldsymbol{F}_{\mathrm{f}} = 2\pi\eta a[3\boldsymbol{\alpha}_1 + \boldsymbol{\beta}_1], \quad \boldsymbol{T}_{\mathrm{f}} = 4\pi\eta a^2 \boldsymbol{\gamma}_1. \tag{3.12a, b}$$

According to arguments in §2, by setting $\boldsymbol{F}_{\mathrm{f}}$ and $\boldsymbol{T}_{\mathrm{f}}$ equal to zero we shall obtain $\boldsymbol{U}$ and $\boldsymbol{\Omega}$.

There is no rotational motion in this problem, because ζ_{p} is constant and the electric field is the gradient of a scalar. After substituting (3.10) into the left-hand side of (3.11c), we have

$$\left.\begin{aligned} 2a\boldsymbol{n}\cdot\boldsymbol{\Omega} &= \sum_{m=1}^{\infty} \boldsymbol{\gamma}_m[\cdot]\boldsymbol{S}_m, \\ \boldsymbol{\gamma}_1 &= -2a\boldsymbol{\Omega}, \\ \boldsymbol{\gamma}_m &= \boldsymbol{0} \quad \text{for } m \neq 1. \end{aligned}\right\} \tag{3.13}$$

By setting $\boldsymbol{T}_{\mathrm{f}} = \boldsymbol{0}$ and using (3.12*b*), we find

$$\boldsymbol{\Omega} = \boldsymbol{0}, \tag{3.14}$$

as a general result for any imposed field $\boldsymbol{E}_{\mathrm{A}}$ as long as $\nabla\cdot\boldsymbol{E}_{\mathrm{A}} = 0$.

The translational motion is described by the coefficients $\boldsymbol{\alpha}_m$ and $\boldsymbol{\beta}_m$. From (3.10) and (3.11*a*) we have

$$\left.\begin{aligned} \boldsymbol{\alpha}_1 &= -\boldsymbol{U}, \\ \boldsymbol{\alpha}_m &= \boldsymbol{0} \quad \text{for } m \neq 1. \end{aligned}\right\} \tag{3.15}$$

Multiplying (3.11*b*) by $\boldsymbol{S}_1 = -\boldsymbol{n}$ and averaging over $r = a^+$, we obtain

$$\boldsymbol{\beta}_1 = \frac{3\epsilon\zeta_{\mathrm{p}}}{4\pi\eta}(\boldsymbol{E}_{\mathrm{A}})_0. \tag{3.16}$$

The particle's translational velocity is found by combining (3.12*a*), (3.15) and (3.16), and then setting $\boldsymbol{F}_{\mathrm{f}} = \boldsymbol{0}$:

$$\boldsymbol{U} = \frac{\epsilon\zeta_{\mathrm{p}}}{4\pi\eta}(\boldsymbol{E}_{\mathrm{A}})_0. \tag{3.17}$$

This result is identical with Smoluchowski's equation, which, to our knowledge, has heretofore only been derived for constant $\boldsymbol{E}_{\mathrm{A}}$. We emphasize that (3.14) and (3.17) are only valid when $\kappa a \gg \cosh(Ze\zeta_{\mathrm{p}}/2kT)$ and ζ_{p} is constant on the particle/fluid interface. Dielectrophoresis ($\boldsymbol{U} \sim \nabla\boldsymbol{E}_{\mathrm{A}}$) occurs only when there is a dipole, that is, ζ_{p} is not uniform (Anderson 1985).

Although non-zero derivatives of the applied field have no effect on the particle velocity, they do contribute to the fluid velocity field through the coefficients $\boldsymbol{\beta}_m$. If terms $O(\nabla\nabla\boldsymbol{E}_{\mathrm{A}})$ are ignored, only $\boldsymbol{\beta}_1$ and $\boldsymbol{\beta}_2$ are needed, with the latter obtained from (3.9), (3.10) and (3.11*b*):

$$\boldsymbol{\beta}_2 = -\tfrac{5}{3}a\left(\frac{\epsilon\zeta_{\mathrm{p}}}{4\pi\eta}\right)(\nabla\boldsymbol{E}_{\mathrm{A}})_0. \tag{3.18}$$

The velocity field about the moving particle is

$$\boldsymbol{v} = \nabla\boldsymbol{\phi}_{-2} + \nabla\boldsymbol{\phi}_{-3} + \frac{1}{2\eta}\boldsymbol{r}\boldsymbol{p}_{-3} + O(\nabla\nabla\boldsymbol{E}_{\mathrm{A}}), \tag{3.19}$$

where the functions $\phi_{-(m+1)}$ and $p_{-(m+1)}$ are given by Brenner (1964*a*) and are $O(r^{-(m+1)})$. After evaluating ϕ_{-2}, ϕ_{-3} and p_{-3} from $\boldsymbol{\alpha}_1$, $\boldsymbol{\beta}_1$ and $\boldsymbol{\beta}_2$, we have

$$v(r) = \frac{\epsilon\zeta_P}{4\pi\eta}\left\{\frac{1}{2}\left(\frac{a}{r}\right)^3\left[3\frac{\boldsymbol{rr}}{r^2}-\boldsymbol{I}\right]\cdot(\boldsymbol{E}_A)_0 - \left[\frac{5}{2}\frac{a^3}{r^5}\boldsymbol{rrr}+\frac{5}{6}\left(\frac{a}{r}\right)^5\left(2\boldsymbol{Ir}-5\frac{\boldsymbol{rrr}}{r^2}\right)\right]:(\nabla\boldsymbol{E}_A)_0+O(\nabla\nabla\boldsymbol{E}_A)\right\}. \quad (3.20)$$

To leading order in electric field, v decays as r^{-3}, rather than as a Stokeslet or force dipole. Such an unbounded velocity field is characteristic of 'phoretic' motions, that is movement caused by conservative forces operating only within a thin fluid region at the surface of a particle (Anderson, Lowell & Prieve 1982; Anderson 1983). Curiously, the $O(\nabla\boldsymbol{E}_A)$ contribution decays more slowly than does the $O(\boldsymbol{E}_A)$ velocity field (r^{-2} versus r^{-3}). This observation is important in §§4 and 5 when computing reflected velocity fields between particle and boundary.

The unbounded velocity field caused by a force-free rigid sphere in an arbitrary undisturbed flow can be determined from the analysis of Brenner (1964*b*). In the analyses of §§4 and 5 the particle disturbance to each wall-reflected electrical potential will be computed from (3.7); while the particle velocity disturbances caused by each wall-reflected potential and velocity field will be computed from (3.20) and Brenner's analysis (1964*b*) respectively.

4. Electrophoresis near single walls

We consider in this section the electrophoretic motion of an insulating sphere of radius a in the direction either parallel or perpendicular to an infinite flat wall located at a distance b from the sphere centre. For the case in which a uniform electric field $-\nabla\Phi_\infty$ is imposed parallel to the plane wall, the wall is assumed to be non-conducting and the boundary condition (2.17) applies; while, for the case where the direction of $-\nabla\Phi_\infty$ is perpendicular to the wall, the wall is assumed perfectly conducting and (2.22) is the appropriate boundary condition as noted in §2. In both cases the sphere centre is chosen to be the origin of the coordinate frame, as shown in figure 2, and the applied electric field is expressed by $E_\infty \boldsymbol{e}_z$. Here (x,y,z), (ρ,ϕ,z) and (r,θ,ϕ) are Cartesian, circular cylindrical and spherical coordinates respectively. The effect of the wall on the electrophoretic velocity of the particle is sought in an expansion of λ, which equals the ratio of particle radius to distance between the wall and centre of the particle.

Motion parallel to an infinite wall

For the problem of electrophoretic motion parallel to an insulating plane wall, as depicted in figure 2(*a*), (2.16) and (2.19) must be solved by satisfying the following conditions derived from (2.9*b*), (2.17), (2.20) and (3.14) when $\kappa a \to \infty$:

$$\left.\begin{aligned} \boldsymbol{e}_r\cdot\nabla\Phi &= 0, && (4.1a)\\ \boldsymbol{v} &= \boldsymbol{U}+\frac{\epsilon\zeta_P}{4\pi\eta}\nabla\Phi && (4.1b)\dagger \end{aligned}\right\} \quad (r=a);$$

$$\left.\begin{aligned} \boldsymbol{e}_x\cdot\nabla\Phi &= 0, && (4.2a)\\ \boldsymbol{v} &= \frac{\epsilon\zeta_W}{4\pi\eta}\nabla\Phi && (4.2b) \end{aligned}\right\} \quad (x=b);$$

† The velocity field reflected from the wall may produce a non-zero $\boldsymbol{\Omega}$, but this free rotation has no effect on $\boldsymbol{U}$.

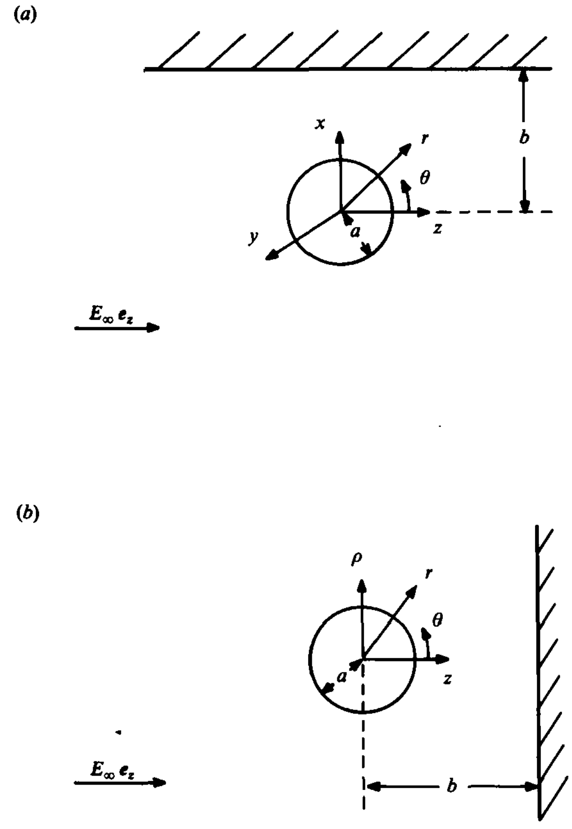

FIGURE 2. Electrophoresis of a spherical particle near single walls: (*a*) motion parallel to an infinite plane; (*b*) motion normal to an infinite plane.

$$\left.\begin{aligned} \Phi &\rightarrow -E_\infty z, \\ \boldsymbol{v} &\rightarrow -\frac{\epsilon\zeta_w}{4\pi\eta}E_\infty \boldsymbol{e}_z \end{aligned}\right\} \quad (r\rightarrow\infty,\ x<b). \qquad \begin{aligned}(4.3a)\\(4.3b)\end{aligned}$$

ζ_p and ζ_w are the zeta potentials of the sphere and of the wall respectively. The far-field condition (4.3 *b*) accounts for the undisturbed electroosmotic velocity of the fluid outside the thin double layer caused by the presence of the charged plane. In this problem, the translational velocity $\boldsymbol{U}$ of the sphere is what we need to evaluate.

For the motion of a uniformly charged sphere under an arbitrary applied electric field $\boldsymbol{E}_A(\boldsymbol{x})$ and velocity field $\boldsymbol{v}_A(\boldsymbol{x})$ in an *unbounded* fluid, $\boldsymbol{U}$ can be found by combining (3.17) and Faxen's law (Happel & Brenner 1973) in the limit of $\kappa a\rightarrow\infty$:

$$\boldsymbol{U} = \frac{\epsilon\zeta_p}{4\pi\eta}(\boldsymbol{E}_A)_0 + (\boldsymbol{v}_A)_0 + \tfrac{1}{6}a^2(\nabla^2\boldsymbol{v}_A)_0, \tag{4.4}$$

where subscript 0 denotes the position of the sphere centre. It is easily demonstrable that Faxen's law (the second and third terms on the right-hand side of (4.4)) applies to a charged sphere in the limit $\kappa a\rightarrow\infty$. The superposition of the electrostatic and hydrodynamic contributions in the above equation is valid because governing equations in the region outside the thin double layer are linear.

In the situation $\lambda = a/b \ll 1$ a method of reflections is used to solve the problem. The solution consists of the following series, whose terms depend on increasing powers of λ:

$$\boldsymbol{\Phi} = \Phi_{\mathrm{w}}^{(0)} + \Phi_{\mathrm{p}}^{(1)} + \Phi_{\mathrm{w}}^{(1)} + \Phi_{\mathrm{p}}^{(2)} + \Phi_{\mathrm{w}}^{(2)} + \dots, \tag{4.5a}$$

$$\boldsymbol{v} = \boldsymbol{v}_{\mathrm{w}}^{(0)} + \boldsymbol{v}_{\mathrm{p}}^{(1)} + \boldsymbol{v}_{\mathrm{w}}^{(1)} + \boldsymbol{v}_{\mathrm{p}}^{(2)} + \boldsymbol{v}_{\mathrm{w}}^{(2)} + \dots, \tag{4.5b}$$

where subscripts w and p represent the reflections from wall and particle respectively, and the superscript (i) denotes the ith reflection from that solid surface (or, more precisely, from the outer edge of the thin double layer). In these series, all the sets of the corresponding electrical potential and velocity must satisfy (2.16) and (2.19). The advantage of this method is that it is necessary to consider boundary conditions associated with only one surface at a time. According to (4.5), the particle velocity can also be expressed in the form of a series

$$\boldsymbol{U} = \boldsymbol{U}^{(0)} + \boldsymbol{U}^{(1)} + \boldsymbol{U}^{(2)} + \dots, \tag{4.6}$$

where each $\boldsymbol{U}^{(i)}$ is related to $\boldsymbol{E}_{\mathrm{w}}^{(i)}$ $(= -\nabla\Phi_{\mathrm{w}}^{(i)})$ and $\boldsymbol{v}_{\mathrm{w}}^{(i)}$ by (4.4), because the fields reflected from the wall can be thought as imposed on the particle in an unbounded medium.

The electric and velocity fields unperturbed by the presence of the particle are

$$\boldsymbol{E}_{\mathrm{w}}^{(0)} = E_\infty \boldsymbol{e}_z, \quad \boldsymbol{v}_{\mathrm{w}}^{(0)} = -\frac{\epsilon\zeta_{\mathrm{w}}}{4\pi\eta} E_\infty \boldsymbol{e}_z, \tag{4.7a, b}$$

which give

$$\boldsymbol{U}^{(0)} = \frac{\epsilon}{4\pi\eta}(\zeta_{\mathrm{p}} - \zeta_{\mathrm{w}}) E_\infty \boldsymbol{e}_z. \tag{4.7c}$$

This result is a superposition of Smoluchowski's relation for electrophoresis and the Helmholtz equation for electro-osmotic flow caused by the charged wall in an 'open' system, that is, no pressure gradients are established to counteract the electro-osmotic flow.

The boundary conditions for the ith reflected fields from the particle are derived from (4.1) and (4.3):

$$\left.\begin{aligned} \boldsymbol{e}_r\cdot\nabla\Phi_{\mathrm{p}}^{(i)} &= -\boldsymbol{e}_r\cdot\nabla\Phi_{\mathrm{w}}^{(i-1)}, && (4.8a)\\ \boldsymbol{v}_{\mathrm{p}}^{(i)} &= -\boldsymbol{v}_{\mathrm{w}}^{(i-1)} + \boldsymbol{U}^{(i-1)} + \frac{\epsilon\zeta_{\mathrm{p}}}{4\pi\eta}\nabla[\Phi_{\mathrm{w}}^{(i-1)} + \Phi_{\mathrm{p}}^{(i)}] && (4.8b) \end{aligned}\right\} \quad (r = a);$$

$$\left.\begin{aligned} \Phi_{\mathrm{p}}^{(i)} &\to 0, && (4.8c)\\ \boldsymbol{v}_{\mathrm{p}}^{(i)} &\to \boldsymbol{0} && (4.8d) \end{aligned}\right\} \quad (r \to \infty);$$

where $i = 1, 2, \dots$. The solution for the first reflected fields, which satisfy (2.16) and (2.19) and the above boundary conditions, is obtained from (3.7) and (3.20):

$$\Phi_{\mathrm{p}}^{(1)} = -\tfrac{1}{2}E_\infty \frac{a^3}{r^2}\cos\theta, \tag{4.9a}$$

$$\boldsymbol{v}_{\mathrm{p}}^{(1)} = U_0\left(\frac{a}{r}\right)^3(\cos\theta\, \boldsymbol{e}_r + \tfrac{1}{2}\sin\theta\, \boldsymbol{e}_\theta), \tag{4.9b}$$

where

$$U_0 = \frac{\epsilon\zeta_{\mathrm{p}}}{4\pi\eta}E_\infty. \tag{4.9c}$$

The velocity distribution shown in (4.9*b*) is an irrotational flow around a sphere moving with velocity $U_0 \boldsymbol{e}_z$.

The boundary conditions for the ith reflected fields from the wall are derived from (4.2) and (4.3):

$$\left.\begin{aligned} \boldsymbol{e}_x \cdot \nabla \Phi_{\mathrm{w}}^{(i)} &= -\boldsymbol{e}_x \cdot \nabla \Phi_{\mathrm{p}}^{(i)}, \\ \boldsymbol{v}_{\mathrm{w}}^{(i)} &= -\boldsymbol{v}_{\mathrm{p}}^{(i)} + \frac{\epsilon \zeta_{\mathrm{w}}}{4\pi\eta} \nabla[\Phi_{\mathrm{p}}^{(i)} + \Phi_{\mathrm{w}}^{(i)}] \end{aligned}\right\} \quad (x = b); \qquad \begin{aligned} &(4.10a) \\ &(4.10b) \end{aligned}$$

$$\left.\begin{aligned} \Phi_{\mathrm{w}}^{(i)} &\to 0, \\ \boldsymbol{v}_{\mathrm{w}}^{(i)} &\to \mathbf{0} \end{aligned}\right\} \quad (r \to \infty,\ x < b). \qquad \begin{aligned} &(4.10c) \\ &(4.10d) \end{aligned}$$

The solution for $\Phi_{\mathrm{w}}^{(1)}$ is obtained by applying complex Fourier transforms on z and y in (2.16) and (4.10*a*, *c*), with the result

$$\Phi_{\mathrm{w}}^{(1)} = -\tfrac{1}{2} E_\infty a^3 z[(2b-x)^2 + y^2 + z^2]^{-\frac{3}{2}}. \tag{4.11a}$$

This reflected electrical potential may be interpreted as arising from the reflection of the imposed field $E_\infty \boldsymbol{e}_z$ from a fictitious sphere equal in size to the actual sphere, its location being at the mirror-image position of the actual sphere with respect to the plane $x = b$ (i.e. at $x = 2b$, $y = 0$, $z = 0$). With knowledge of $\boldsymbol{v}_{\mathrm{p}}^{(1)}$, $\Phi_{\mathrm{p}}^{(1)}$ and $\Phi_{\mathrm{w}}^{(1)}$, $\boldsymbol{v}_{\mathrm{w}}^{(1)}$ can be found by fitting the boundary conditions (4.10*b*, *d*) with the general solution of (2.19) established by Faxen (see Happel & Brenner 1973, p. 323), which results in

$$\begin{aligned} \boldsymbol{v}_{\mathrm{w}}^{(1)} = \frac{U_0 a^3}{4\pi} \int_{-\infty}^{+\infty} \int_{-\infty}^{+\infty} \mathrm{e}^{\mathrm{i}(\alpha y + \beta z) - m(2b-x)} \Big\{ &[1 + 2(1-\gamma)(mb - mx)]\, \mathrm{i}\beta \boldsymbol{e}_x \\ &- [1 + 2(1-\gamma)(mb - mx - 1)] \left(\frac{\alpha\beta}{m} \boldsymbol{e}_y + \frac{\beta^2}{m} \boldsymbol{e}_z \right) \Big\} \,\mathrm{d}\alpha\, \mathrm{d}\beta, \end{aligned} \tag{4.11b}$$

where $\gamma = \zeta_{\mathrm{w}}/\zeta_{\mathrm{p}}$, $m = (\alpha^2 + \beta^2)^{\frac{1}{2}}$ and $\mathrm{i} = \sqrt{-1}$.

The contributions of $\Phi_{\mathrm{w}}^{(1)}$ and $\boldsymbol{v}_{\mathrm{w}}^{(1)}$ to the particle velocity are determined using (4.4):

$$\boldsymbol{U}_{\mathrm{e}}^{(1)} = \frac{\epsilon \zeta_{\mathrm{p}}}{4\pi\eta} [-\nabla \Phi_{\mathrm{w}}^{(1)}]_{r=0} = \tfrac{1}{16} \lambda^3 U_0 \boldsymbol{e}_z, \tag{4.12a}$$

$$\boldsymbol{U}_{\mathrm{h}}^{(1)} = [\boldsymbol{v}_{\mathrm{w}}^{(1)} + \tfrac{1}{6} a^2 \nabla^2 \boldsymbol{v}_{\mathrm{w}}^{(1)}]_{r=0} = [(-\tfrac{1}{8} + \tfrac{1}{16}\gamma)\lambda^3 + \tfrac{1}{8}(1-\gamma)\lambda^5]\, U_0 \boldsymbol{e}_z \tag{4.12b}$$

and

$$\boldsymbol{U}^{(1)} = \boldsymbol{U}_{\mathrm{e}}^{(1)} + \boldsymbol{U}_{\mathrm{h}}^{(1)} = (-\tfrac{1}{16}\lambda^3 + \tfrac{1}{8}\lambda^5) \frac{\epsilon}{4\pi\eta} (\zeta_{\mathrm{p}} - \zeta_{\mathrm{w}}) E_\infty \boldsymbol{e}_z. \tag{4.12c}$$

Note that the reflected electrical potential from the wall *increases* the electrophoretic velocity of the particle, while the reflected velocity field tends to *decrease* the magnitude of the particle velocity. Also, the wall correction to the sphere velocity is found to be $O(\lambda^3)$, which is different from that obtained for the sedimentation problem, in which the leading wall correction is $O(\lambda)$.

Substituting the results of first reflection into the boundary conditions (4.8), the second reflected electrical potential and velocity fields from the particle are obtained using (3.7), (3.20) and the derivation by Brenner (1964*b*):

$$\Phi_{\mathrm{p}}^{(2)} = E_\infty[-\tfrac{1}{32}\lambda^3 a^3 r^{-2} \cos\theta - \tfrac{1}{16}\lambda^4 a^4 r^{-3} \cos\theta \sin\theta \cos\phi + O(\lambda^5 a^5)], \tag{4.13a}$$

$$\begin{aligned} \boldsymbol{v}_{\mathrm{p}}^{(2)} = U_0[&\tfrac{1}{16}\lambda^3 a^3 r^{-3} (\cos\theta\, \boldsymbol{e}_r + \tfrac{1}{2} \sin\theta\, \boldsymbol{e}_\theta) \\ &+ \tfrac{15}{16}(1-\gamma)\lambda^4 a^2 r^{-2} \cos\theta \sin\theta \cos\phi\, \boldsymbol{e}_r + O(\lambda^4 a^4, \lambda^5 a^3)]. \end{aligned} \tag{4.13b}$$

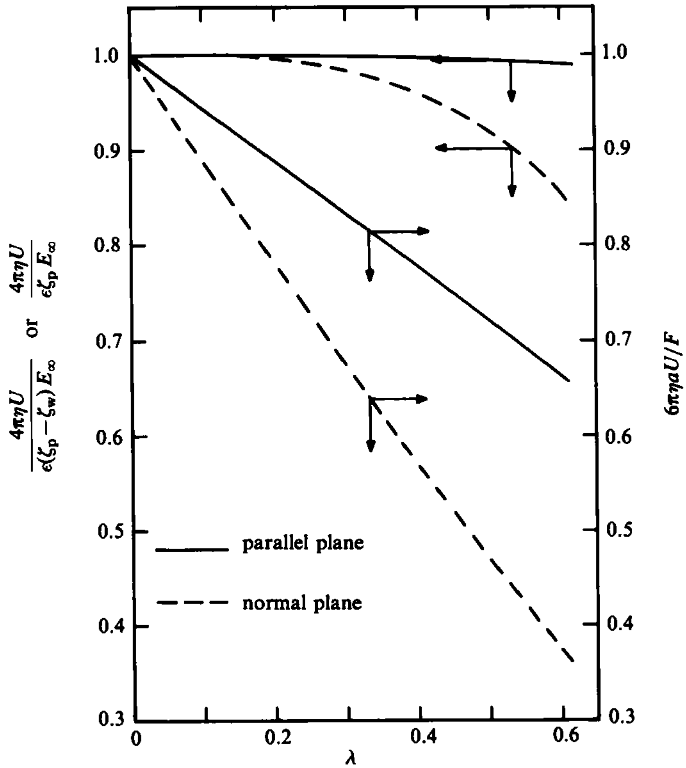

FIGURE 3. Normalized electrophoretic mobility (as computed from (4.16) and (4.26)) and Stokes mobility (as obtained from (4.17) and Brenner 1961) of a sphere near single plane walls.

Here the $\lambda^4 a^2$ term in (4.13*b*) results from the contribution of the $O(\nabla E_w^{(1)})$ field according to (3.20).

The boundary conditions on the second reflected fields from the wall are obtained by substituting the results for $\Phi_p^{(2)}$ and $v_p^{(2)}$ into (4.10), with which (2.16) and (2.19) can be solved as before to give the following:

$$E_w^{(2)} = (\tfrac{1}{16}\lambda^3)^2 E_\infty e_z + O(\lambda^7), \tag{4.14a}$$

$$v_w^{(2)} = (-\tfrac{1}{8}+\tfrac{31}{256}\gamma)\lambda^6 U_0 e_z + O(\lambda^7). \tag{4.14b}$$

The contribution of the second reflected fields to the particle velocity is obtained by putting $E_w^{(2)}$ and $v_w^{(2)}$ into (4.4), which gives

$$U^{(2)} = [-\tfrac{31}{256}\lambda^6 + O(\lambda^8)]\frac{\epsilon}{4\pi\eta}(\zeta_p - \zeta_w)E_\infty e_z. \tag{4.15}$$

The error is $O(\lambda^8)$ because the $O(\lambda^7)$ terms in the expansions of $E_w^{(2)}$ and $v_w^{(2)}$ vanish at the centre of the particle.

With the combination of (4.7*c*), (4.12*c*) and (4.15), the particle velocity can be expressed as

$$U = [1 - \tfrac{1}{16}\lambda^3 + \tfrac{1}{8}\lambda^5 - \tfrac{31}{256}\lambda^6 + O(\lambda^8)]\frac{\epsilon}{4\pi\eta}(\zeta_p - \zeta_w)E_\infty e_z. \tag{4.16}$$

The wall does not deflect the direction of electrophoresis; rather, the particle moves either with or against the applied electric field, depending only on the zeta potential difference between the particle and the wall, at a rate that decreases as the particle approaches the wall ($\lambda \rightarrow 1$).

For the motion of a sphere on which a constant force Fe_z (e.g. a gravitational field) is applied parallel to a plane wall, Faxen obtained the following expression for the particle velocity (see Happel & Brenner 1973, p. 327):

$$U = [1-\tfrac{9}{16}\lambda+\tfrac{1}{8}\lambda^3-\tfrac{45}{256}\lambda^4-\tfrac{1}{16}\lambda^5+O(\lambda^6)]\frac{1}{6\pi\eta a}Fe_z. \tag{4.17}$$

Figure 3 gives a comparison between (4.16) and (4.17). Obviously, the wall effect on electrophoresis is much weaker than that on a sedimenting particle.

Motion normal to an infinite plane wall

Consider the electrophoresis of non-conducting sphere normal to a perfectly conducting plane wall, as shown in figure 2(*b*). We need to solve (2.16) and (2.19) with the boundary conditions given in (4.1), and with (4.2) and (4.3) replaced by

$$\left.\begin{aligned} \Phi &= -E_\infty b, & (4.18a)\\ v &= \mathbf{0} & (4.18b)\end{aligned}\right\} \quad (z=b);$$

$$\left.\begin{aligned} \Phi &\rightarrow -E_\infty z, & (4.18c)\\ v &\rightarrow \mathbf{0} & (4.18d)\end{aligned}\right\} \quad (r\rightarrow\infty,\ z\leqslant b).$$

The condition (4.18*a*) results from (2.22) and (4.18*c*), and (4.18*b*) is derived from (2.20*b*). There is no electrokinetic tangential velocity at the plane wall because there is no tangential component of electric field. In this problem, all the ϕ-dependent terms in the equations vanish because of axial symmetry.

When $\lambda = a/b \ll 1$, the method of reflections can also be used. With the series expansions of electrical potential and velocity in (4.5) and the particle velocity in (4.6), it can be found that

$$\Phi_{\mathrm{w}}^{(0)} = -E_\infty z, \quad v_{\mathrm{w}}^{(0)} = \mathbf{0} \tag{4.19a, b}$$

and

$$U^{(0)} = \frac{\epsilon\zeta_{\mathrm{p}}}{4\pi\eta}E_\infty e_z. \tag{4.19c}$$

The boundary conditions for the ith reflected electrical potential and velocity fields from the particle, given in (4.8) and the solution of $\Phi_{\mathrm{p}}^{(1)}$ and $v_{\mathrm{p}}^{(1)}$ in (4.9), are still valid here, but the boundary conditions for the ith reflected fields from the plane wall differ from the previous situation because the electrical potential on the wall is uniform:

$$\left.\begin{aligned} \Phi_{\mathrm{w}}^{(i)} &= -\Phi_{\mathrm{p}}^{(i)}, & (4.20a)\\ v_{\mathrm{w}}^{(i)} &= -v_{\mathrm{p}}^{(i)} & (4.20b)\end{aligned}\right\} \quad (z=b);$$

$$\left.\begin{aligned} \Phi_{\mathrm{w}}^{(i)} &\rightarrow 0, & (4.20c)\\ v_{\mathrm{w}}^{(i)} &\rightarrow \mathbf{0} & (4.20d)\end{aligned}\right\} \quad (r\rightarrow\infty,\ z\leqslant b).$$

The solution for $\Phi_{\mathrm{w}}^{(1)}$ can be obtained by applying Hankel transforms on the variable ρ in (2.16) and (4.20), with the result

$$\Phi_{\mathrm{w}}^{(1)} = \tfrac{1}{2}E_\infty a^3(2b-z)[(2b-z)^2+\rho^2]^{-\frac{3}{2}}, \tag{4.21a}$$

and $\boldsymbol{v}_{\mathrm{w}}^{(1)}$ can also be solved by applying Hankel transforms (twice) to the Stokes equation in the form of the stream function (as used by Sonshine, Cox & Brenner 1966), which results in

$$\begin{aligned}\boldsymbol{v}_{\mathrm{w}}^{(1)} = U_0 a^3 \{&(-[(2b-z)^2+\rho^2]^{-\frac{3}{2}}+[\tfrac{3}{2}\rho^2-6(b-z)(2b-z)][(2b-z)^2+\rho^2]^{-\frac{5}{2}} \\ &+15\rho^2(b-z)(2b-z)[(2b-z)^2+\rho^2]^{-\frac{7}{2}})\,\boldsymbol{e}_z+(-\tfrac{3}{2}\rho(4b-3z)[(2b-z)^2+\rho^2]^{-\frac{5}{2}} \\ &+15\rho(b-z)(2b-z)^2[(2b-z)^2+\rho^2]^{-\frac{7}{2}})\,\boldsymbol{e}_\rho\}. \end{aligned} \tag{4.21b}$$

Substituting $\Phi_{\mathrm{w}}^{(1)}$ and $\boldsymbol{v}_{\mathrm{w}}^{(1)}$ into (4.4), we have

$$\frac{\epsilon\zeta_{\mathrm{p}}}{4\pi\eta}[-\nabla\Phi_{\mathrm{w}}^{(1)}]_{r=0} = -\tfrac{1}{8}\lambda^3 U_0\,\boldsymbol{e}_z, \tag{4.22a}$$

$$[\boldsymbol{v}_{\mathrm{w}}^{(1)}+\tfrac{1}{6}a^2\nabla^2\boldsymbol{v}_{\mathrm{w}}^{(1)}]_{r=0} = [-\tfrac{1}{2}\lambda^3+\tfrac{1}{4}\lambda^5]\,U_0\,\boldsymbol{e}_z, \tag{4.22b}$$

or

$$\boldsymbol{U}^{(1)} = [-\tfrac{5}{8}\lambda^3+\tfrac{1}{4}\lambda^5]\frac{\epsilon\zeta_{\mathrm{p}}}{4\pi\eta}E_\infty\,\boldsymbol{e}_z. \tag{4.22c}$$

Note that the reflected electric field reduces the particle velocity in this case, which is opposite to the effect of a non-conducting parallel wall.

In a similar way to the previous case, the results of the second reflection can be obtained with knowledge of the first reflection, and are summarized as follows:

$$\Phi_{\mathrm{p}}^{(2)} = E_\infty[\tfrac{1}{16}\lambda^3a^3r^{-2}\cos\theta+\tfrac{1}{32}\lambda^4a^4r^{-3}(3\cos^2\theta-1)+O(\lambda^5a^5)], \tag{4.23a}$$

$$\begin{aligned}\boldsymbol{v}_{\mathrm{p}}^{(2)} = U_0[&-\tfrac{1}{8}\lambda^3a^3r^{-3}(\cos\theta\,\boldsymbol{e}_r+\tfrac{1}{2}\sin\theta\,\boldsymbol{e}_\theta) \\ &+\tfrac{15}{16}\lambda^4a^2r^{-2}(3\cos^2\theta-1)\,\boldsymbol{e}_r+O(\lambda^4a^4,\lambda^5a^3)], \end{aligned} \tag{4.23b}$$

$$\boldsymbol{E}_{\mathrm{w}}^{(2)} = \tfrac{1}{64}\lambda^6E_\infty\,\boldsymbol{e}_z+O(\lambda^7), \quad \boldsymbol{v}_{\mathrm{w}}^{(2)} = -\tfrac{41}{64}\lambda^6U_0\,\boldsymbol{e}_z+O(\lambda^7) \tag{4.24a, b}$$

and

$$\boldsymbol{U}^{(2)} = [-\tfrac{5}{8}\lambda^6+O(\lambda^8)]\frac{\epsilon\zeta_{\mathrm{p}}}{4\pi\eta}E_\infty\boldsymbol{e}_z. \tag{4.25}$$

The combination of (4.19*c*), (4.22*c*) and (4.25) gives the following expression for the wall-corrected electrophoretic velocity:

$$\boldsymbol{U} = [1-\tfrac{5}{8}\lambda^3+\tfrac{1}{4}\lambda^5-\tfrac{5}{8}\lambda^6+O(\lambda^8)]\frac{\epsilon\zeta_{\mathrm{p}}}{4\pi\eta}E_\infty\,\boldsymbol{e}_z. \tag{4.26}$$

For the motion of a sphere perpendicular to a plane wall caused by a constant force $F\boldsymbol{e}_z$, the exact result of the particle velocity was developed by Brenner (1961). A comparison between this Stokes' law correction and (4.26) is given in figure 3.

5. Electrophoresis in long pores

Considered in this section is the electrophoresis of a non-conducting sphere in an infinitely long pore. The pore is assumed to be either a circular cylinder of radius R or a slit of half-width B; the pore walls are considered to be non-conducting. The sphere's centre is still chosen to be the origin of the coordinate system, and the sphere moves along the axis of the cylinder (as shown in figure 4*a*) or in the central plane of the slit (as shown in figure 4*b*) under a uniform imposed electric field $E_\infty\,\boldsymbol{e}_z$.

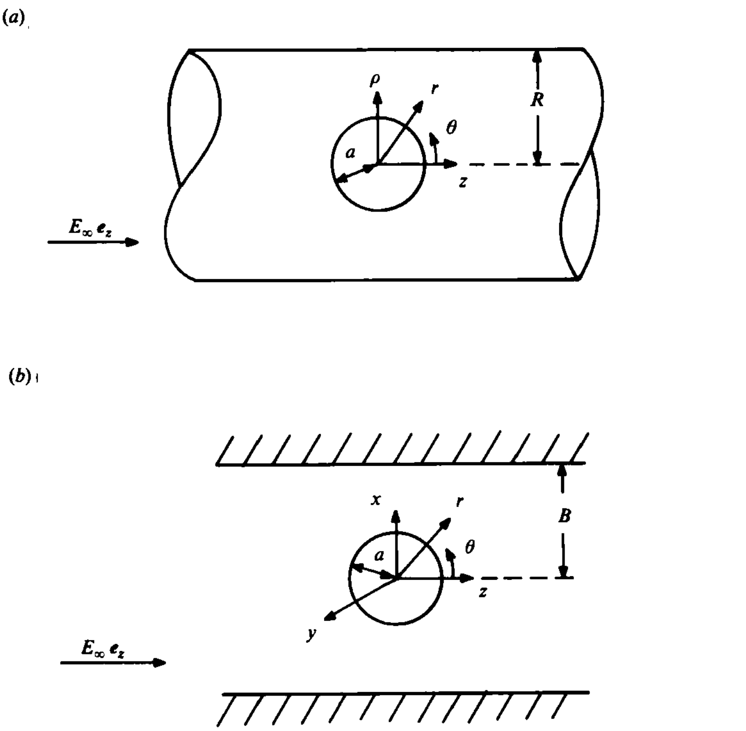

FIGURE 4. Electrophoresis of a spherical particle along the axis of infinitely long pores: (*a*) circular cylinder; (*b*) slit.

Slit pore

For the problem of electrophoresis in the midplane between two parallel walls (figure 4*b*), the boundary conditions corresponding to governing equations (2.16) and (2.19) are given by (4.1) and the following:

$$\left.\begin{aligned} \boldsymbol{e}_x\cdot\nabla\Phi &= 0, \qquad &(5.1a)\\ \boldsymbol{v} &= \frac{\epsilon\zeta_{\mathrm{w}}}{4ph}\nabla\Phi \qquad &(5.1b)\end{aligned}\right\}\quad (|x| = B);$$

$$\left.\begin{aligned} \Phi &\to -E_\infty z, \qquad &(5.2a)\\ \boldsymbol{v} &\to -\frac{\epsilon\zeta_{\mathrm{w}}}{4\pi\eta}E_\infty\boldsymbol{e}_z \qquad &(5.2b)\end{aligned}\right\}\quad (r\to\infty,\ |x| < B).$$

Letting $\lambda = a/B \leqslant 1$, the method of reflections employed in §4 can also be used to solve this problem. Using a series expansion of the same form as (4.5)–(4.6), it can be shown that the unreflected fields described by (4.7), the boundary conditions for the reflected fields from the particle in (4.8), and the first reflected fields in (4.9) are all valid here. The boundary conditions for the *i*th reflected fields from the wall are derived from (5.1) and (5.2):

$$\left.\begin{aligned} \boldsymbol{e}_x\cdot\nabla\Phi_{\mathrm{w}}^{(i)} &= -\boldsymbol{e}_x\cdot\nabla\Phi_{\mathrm{p}}^{(i)} \qquad &(5.3a)\\ \boldsymbol{v}_{\mathrm{w}}^{(i)} &= -\boldsymbol{v}_{\mathrm{p}}^{(i)}+\frac{\epsilon\zeta_{\mathrm{w}}}{4\pi\eta}\nabla[\Phi_{\mathrm{p}}^{(i)}+\Phi_{\mathrm{w}}^{(i)}] \qquad &(5.3b)\end{aligned}\right\}\quad (|x| = B);$$

$$\left.\begin{aligned} \Phi_{\mathrm{w}}^{(i)} &\rightarrow 0, \\ \boldsymbol{v}_{\mathrm{w}}^{(i)} &\rightarrow \mathbf{0} \end{aligned}\right\} \quad (r \rightarrow \infty,\ |x| < B). \tag{5.3c, d}$$

Then the first reflected fields can be solved by the same method as used for a single parallel wall in §4 with the results

$$\Phi_{\mathrm{w}}^{(1)} = \frac{E_{\infty} a^3}{4\pi} \int_{-\infty}^{+\infty} \int_{-\infty}^{+\infty} \frac{\mathrm{i}\beta}{m} \mathrm{e}^{\mathrm{i}(\alpha y+\beta z)-mB} \frac{\cosh(mx)}{\sinh(mB)} \,\mathrm{d}\alpha\, \mathrm{d}\beta, \tag{5.4a}$$

$$\begin{aligned} \boldsymbol{v}_{\mathrm{w}}^{(1)} = \frac{U_0 a^3}{2\pi} \int_{-\infty}^{+\infty} \int_{-\infty}^{+\infty} & \frac{1}{\sinh(2mB)-2mB} \mathrm{e}^{\mathrm{i}(\alpha y+\beta z)} \\ & \times \Big\{ \mathrm{i}\beta [(1-\gamma)\sinh(mx) - (1-\gamma)\, mx \cosh(mx) + g \sinh(mx)]\, \boldsymbol{e}_x \\ & + [(1-\gamma)\, mx \sinh(mx) - g\cosh(mx)] \left(\frac{\beta^2}{m}\boldsymbol{e}_z + \frac{\alpha\beta}{m}\boldsymbol{e}_y\right)\Big\} \,\mathrm{d}\alpha\, \mathrm{d}\beta, \end{aligned} \tag{5.4b}$$

where

$$\gamma = \zeta_{\mathrm{w}}/\zeta_{\mathrm{p}}, \quad m = (\alpha^2+\beta^2)^{\frac{1}{2}} \quad \text{and} \quad g = mB - \tfrac{1}{2}(1-\mathrm{e}^{-2mB}) + \gamma - \gamma mB \coth(mB).$$

Substituting $\Phi_{\mathrm{w}}^{(1)}$ and $\boldsymbol{v}_{\mathrm{w}}^{(1)}$ into (4.4) and utilizing the Gauss–Laguerre quadrature for the numerical integrations, we obtain the contributions to the particle velocity due to first wall-reflected fields:

$$\frac{\epsilon\zeta_{\mathrm{p}}}{4\pi\eta}[-\nabla\Phi_{\mathrm{w}}^{(1)}]_{r=0} = d_1 \lambda^3 U_0 \boldsymbol{e}_z, \tag{5.5a}$$

$$[\boldsymbol{v}_{\mathrm{w}}^{(1)} + \tfrac{1}{6}a^2 \nabla^2 \boldsymbol{v}_{\mathrm{w}}^{(1)}]_{r=0} = \{[-d_1 + d_2(1-\gamma)]\lambda^3 + d_3(1-\gamma)\lambda^5\}\, U_0 \boldsymbol{e}_z, \tag{5.5b}$$

which add to give $$\boldsymbol{U}^{(1)} = (d_2\lambda^3 + d_3\lambda^5)\frac{\epsilon}{4\pi\eta}(\zeta_{\mathrm{p}} - \zeta_{\mathrm{w}}) E_{\infty} \boldsymbol{e}_z. \tag{5.5c}$$

Here $$d_1 = \frac{1}{8}\sum_{n=1}^{\infty} n^{-3} = 0.150257,$$

$$d_2 = \frac{1}{2}\int_0^{\infty} \frac{\rho^2(1-\rho\coth\rho)}{\sinh(2\rho)-2\rho}\,\mathrm{d}\rho = -0.267699,$$

$$d_3 = \frac{1}{6}\int_0^{\infty} \frac{\rho^4}{\sinh(2\rho)-2\rho}\,\mathrm{d}\rho = 0.338324.$$

Using the methods of §4 the second reflections are obtained:

$$\Phi_{\mathrm{p}}^{(2)} = -\tfrac{1}{2}d_1\lambda^3 E_{\infty} a^3 r^{-2}\cos\theta + O(\lambda^5 a^5), \tag{5.6a}$$

$$\boldsymbol{v}_{\mathrm{p}}^{(2)} = d_1\lambda^3 U_0 a^3 r^{-3}(\cos\theta\, \boldsymbol{e}_r + \tfrac{1}{2}\sin\theta\, \boldsymbol{e}_\theta) + O(\lambda^5 a^3), \tag{5.6b}$$

$$\boldsymbol{E}_{\mathrm{w}}^{(2)} = (d_1\lambda^3)^2 E_{\infty}\boldsymbol{e}_z + O(\lambda^8), \tag{5.7a}$$

$$\boldsymbol{v}_{\mathrm{w}}^{(2)} = d_1\lambda^3[-d_1 + d_2(1-\gamma)]\lambda^3 U_0 \boldsymbol{e}_z + O(\lambda^8) \tag{5.7b}$$

and $$\boldsymbol{U}^{(2)} = [(d_1\lambda^3)(d_2\lambda^3) + O(\lambda^8)]\frac{\epsilon}{4\pi\eta}(\zeta_{\mathrm{p}} - \zeta_{\mathrm{w}}) E_{\infty}\boldsymbol{e}_z. \tag{5.8}$$

Combination of (4.7c), (5.5c) and (5.8) gives the wall-corrected particle velocity:

$$\boldsymbol{U} = [1 - 0.267699\lambda^3 + 0.338324\lambda^5 - 0.040224\lambda^6 + O(\lambda^8)]\frac{\epsilon}{4\pi\eta}(\zeta_{\mathrm{p}} - \zeta_{\mathrm{w}}) E_{\infty}\boldsymbol{e}_z. \tag{5.9}$$

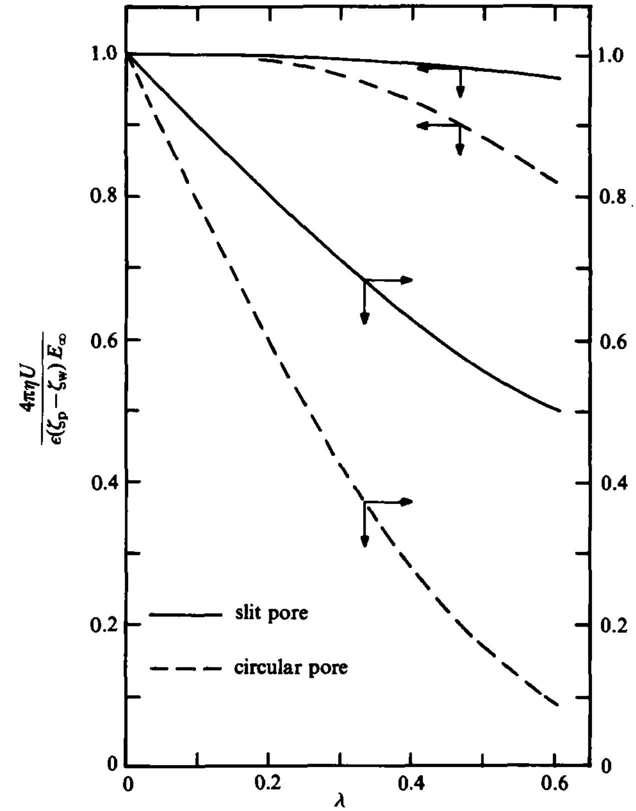

FIGURE 5. Normalized electrophoretic mobility (as computed from equations (5.9) and (5.19)) and Stokes mobility (as obtained from (5.10) and Happel & Brenner 1973, p. 318) of a sphere on the axis of infinitely long pores.

Faxen obtained the following correction to Stokes' law for a sphere moving on the central plane of a slit (Happel & Brenner 1973, p. 327):

$$U = [1-1.004\lambda+0.418\lambda^3+0.21\lambda^4-0.169\lambda^5+O(\lambda^6)]\frac{1}{6\pi\eta a}F\boldsymbol{e}_z. \tag{5.10}$$

Figure 5 shows the difference between (5.9) and (5.10) to compare the wall corrections. Obviously the wall effect in electrophoresis is much weaker. Comparing (5.9) and (5.10) for the slit case with (4.16) and (4.17) for the case of a single wall, we find that the assumption that the results for two walls can be obtained by simple addition of the single-wall effect gives too small a correction to electrophoresis, while for the sedimentation problem this approximation overestimates the wall correction.

Circular cylindrical pore

Consider the electrophoresis of a sphere along the axis of a long circular cylinder, as shown in figure 4(*a*). There is no ϕ-dependence in any of the fields because of axial symmetry. We need to solve (2.16) and (2.19) subject to the boundary conditions given in (4.1) and the following:

$$\left.\begin{aligned} \boldsymbol{e}_\rho\cdot\nabla\Phi &= 0, \qquad &(5.11a)\\ \boldsymbol{v} &= \frac{\epsilon\zeta_w}{4\pi\eta}\nabla\Phi \qquad &(5.11b)\end{aligned}\right\}\quad (\rho = R);$$

$$\left.\begin{aligned} \Phi &\rightarrow -E_\infty z, \\ \boldsymbol{v} &\rightarrow -\frac{\epsilon\zeta_{\mathrm{w}}}{4\pi\eta} E_\infty \boldsymbol{e}_z \end{aligned}\right\} \quad (|z| \rightarrow \infty). \tag{5.12a, b}$$

With $\lambda = a/R \leqslant 1$ (4.5)–(4.9) remain valid here. From (5.11) and (5.12), the boundary conditions for $\Phi_{\mathrm{w}}^{(i)}$ and $\boldsymbol{v}_{\mathrm{w}}^{(i)}$ are found to be

$$\left.\begin{aligned} \boldsymbol{e}_\rho \cdot \nabla \Phi_{\mathrm{w}}^{(i)} &= -\boldsymbol{e}_\rho \cdot \nabla \Phi_{\mathrm{p}}^{(i)} \\ \boldsymbol{v}_{\mathrm{w}}^{(i)} &= -\boldsymbol{v}_{\mathrm{p}}^{(i)} + \frac{\epsilon\zeta_{\mathrm{w}}}{4\pi\eta} \nabla[\Phi_{\mathrm{p}}^{(i)} + \Phi_{\mathrm{w}}^{(i)}] \end{aligned}\right\} \quad (\rho = R); \tag{5.13a, b}$$

$$\left.\begin{aligned} \Phi_{\mathrm{w}}^{(i)} &\rightarrow 0, \\ \boldsymbol{v}_{\mathrm{w}}^{(i)} &\rightarrow \mathbf{0} \end{aligned}\right\} \quad (|z| \rightarrow \infty). \tag{5.13c, d}$$

The solution for the first reflected electrical potential from the cylinder wall can be obtained by applying Fourier sine transforms on the variable z in (2.16) and (5.13a, c), and the result is

$$\Phi_{\mathrm{w}}^{(1)} = -\frac{E_\infty a \lambda^2}{\pi} \int_0^\infty \omega \frac{K_1(\omega)}{I_1(\omega)} I_0\left(\frac{\rho}{R}\omega\right) \sin\left(\frac{z}{R}\omega\right) \mathrm{d}\omega, \tag{5.14a}$$

where $I_n(\omega)$ and $K_n(\omega)$ are modified Bessel functions of the first and second kind respectively. The first wall-reflected velocity field can be solved by applying Fourier cosine transforms (twice) on the variable z in the Stokes equation and boundary conditions (5.13b, d) in the form of a stream function. The result is

$$\begin{aligned} \boldsymbol{v}_{\mathrm{w}}^{(1)} = \frac{U_0 \lambda^3}{\pi} \int_0^\infty \Big\{ & \Big[2A_1(\omega) I_0\left(\frac{\rho}{R}\omega\right) + A_1(\omega) \frac{\rho}{R}\omega I_1\left(\frac{\rho}{R}\omega\right) + A_2(\omega) I_0\left(\frac{\rho}{R}\omega\right)\Big] \cos\left(\frac{z}{R}\omega\right) \boldsymbol{e}_z \\ & + \Big[A_1(\omega) \frac{\rho}{R}\omega I_0\left(\frac{\rho}{R}\omega\right) + A_2(\omega) I_1\left(\frac{\rho}{R}\omega\right)\Big] \sin\left(\frac{z}{R}\omega\right) \boldsymbol{e}_\rho \Big\} \mathrm{d}\omega, \end{aligned} \tag{5.14b}$$

with

$$A_1(\omega) = \frac{1-\gamma}{[I_1(\omega)]^2 - I_0(\omega) I_2(\omega)},$$

$$A_2(\omega) = \frac{-\omega^2[I_1(\omega) K_1(\omega) + I_0(\omega) K_2(\omega)] + \gamma\omega I_0(\omega) [I_1(\omega)]^{-1}}{[I_1(\omega)]^2 - I_0(\omega) I_2(\omega)}.$$

Using the Gauss–Laguerre quadrature, we obtain

$$\frac{\epsilon\zeta_{\mathrm{p}}}{4\pi\eta}[-\nabla\Phi_{\mathrm{w}}^{(1)}]_{r=0} = d_4 \lambda^3 U_0 \boldsymbol{e}_z, \tag{5.15a}$$

$$[\boldsymbol{v}_{\mathrm{w}}^{(1)} + \tfrac{1}{6}a^2 \nabla^2 \boldsymbol{v}_{\mathrm{w}}^{(1)}]_{r=0} = [[-d_4 + d_5(1-\gamma)]\lambda^3 + d_6(1-\gamma)\lambda^5] U_0 \boldsymbol{e}_z, \tag{5.15b}$$

where

$$d_4 = \frac{1}{\pi}\int_0^\infty \omega^2 \frac{K_1(\omega)}{I_1(\omega)} \mathrm{d}\omega = 0.79683,$$

$$d_5 = \frac{1}{\pi}\int_0^\infty \frac{2 - \omega I_0(\omega)[I_1(\omega)]^{-1}}{[I_1(\omega)]^2 - I_0(\omega) I_2(\omega)} \mathrm{d}\omega = -1.28987,$$

$$d_6 = \frac{1}{3\pi}\int_0^\infty \frac{\omega^2}{[I_1(\omega)]^2 - I_0(\omega) I_2(\omega)} \mathrm{d}\omega = 1.89632.$$

$U^{(1)}$ is found by substituting the above equations into (4.4):

$$U^{(1)} = (d_5\lambda^3 + d_6\lambda^5)\frac{\epsilon}{4\pi\eta}(\zeta_p - \zeta_w)E_\infty \boldsymbol{e}_z. \tag{5.15c}$$

The results of second reflection are obtained by using (3.7), (3.20) and Brenner's (1964*b*) analysis for the second particle disturbances, and Fourier sine and cosine transforms on z for the second wall disturbances. The results are

$$\Phi_p^{(2)} = -\tfrac{1}{2}d_4\lambda^3 E_\infty a^3 r^{-2}\cos\theta + O(\lambda^5 a^5), \tag{5.16a}$$

$$v_p^{(2)} = d_4\lambda^3 U_0 a^3 r^{-3}(\cos\theta\,\boldsymbol{e}_r + \tfrac{1}{2}\sin\theta\,\boldsymbol{e}_\theta) + O(\lambda^5 a^3), \tag{5.16b}$$

$$E_w^{(2)} = (d_4\lambda^3)^2 E_\infty \boldsymbol{e}_z + O(\lambda^8), \tag{5.17a}$$

$$v_w^{(2)} = d_4\lambda^3[-d_4 + d_5(1-\gamma)]\lambda^3 U_0 \boldsymbol{e}_z + O(\lambda^8) \tag{5.17b}$$

and

$$U^{(2)} = [(d_4\lambda^3)(d_5\lambda^3) + O(\lambda^8)]\frac{\epsilon}{4\pi\eta}(\zeta_p - \zeta_w)E_\infty \boldsymbol{e}_z. \tag{5.18}$$

The wall-corrected particle velocity that results from the addition of equations (4.7*c*), (5.15*c*) and (5.18) is

$$U = [1 - 1.289\,87\lambda^3 + 1.896\,32\lambda^5 - 1.027\,80\lambda^6 + O(\lambda^8)]\frac{\epsilon}{4\pi\eta}(\zeta_p - \zeta_w)E_\infty \boldsymbol{e}_z. \tag{5.19}$$

The wall effect of a circular pore is significantly greater than for a slit (see (5.9)). A comparison between the well-known Stokes' law correction for a sphere translating along the cylinder axis (Happel & Brenner 1973, p. 318) and (5.19) is made in figure 5. Again, the wall effect on sedimentation is much greater.

6. Discussion

Boundary effects on electrophoresis in the limit $\kappa a \to \infty$ are much weaker than for sedimentation. As seen in (4.16), (4.26), (5.9) and (5.19), the leading order is λ^3, compared with λ for sedimentation. Figures 3 and 5 make the comparison obvious. The reason for the weaker boundary effect on electrophoresis is that the disturbance to both the applied electric field and the fluid velocity field caused by the moving particle in an unbounded fluid decay as r^{-3} (see (3.8) and (3.20)) instead of as a Stokeslet (r^{-1}) characteristic of a particle moving under the influence of a body force. Electrophoresis is an example of 'phoretic motion', which also includes thermocapillary motion of fluid drops (Young, Goldstein & Block 1959), diffusiophoresis of solid particles (Anderson *et al.* 1982; Prieve *et al.* 1984) and osmophoresis of vesicles (Anderson 1983). All such motions result from an interaction between an applied field and a thin fluid layer at the surface of the particle. Outside this layer there is no interaction with the applied field, and hence the hydrodynamic force on an imaginary boundary enclosing the particle plus interfacial layer must be zero. This leads to an r^{-n} decay of the fluid velocity about a moving particle with $n \geqslant 2$; spherical symmetry with a constant applied field requires $n = 3$.

Another peculiarity of electrophoresis in bounded fluids is the existence of electro-osmotic flow (Adamson 1982) due to the interaction between the applied field and the boundary in the absence of the sphere. This effect is expressed by the $-\zeta_w$ term in the $O(\lambda^0)$ coefficient of (4.16), (5.9) and (5.19). Note that the direction of particle motion is determined by the difference in zeta potentials $\zeta_p - \zeta_w$. These equations apply to an *open* system in which there are no pressure gradients established far from the particle; that is, a net electro-osmotic flow is allowed to occur. In electrophoretic experiments, however, the system is usually closed such that the mean fluid flow is zero. To achieve this condition, pressure gradients arise to force the fluid against the electro-osmotic flow and hence the velocity field in the *absence* of the particle can be complex (Hunter 1981). The effect of this pressure-driven 'backflow' on particle velocity must be assessed for the particular geometric configuration of the apparatus or porous medium. Such questions of how to apply the hydrodynamic results of this paper to interpret actual electrophoretic data or to predict particle fluxes due to electrophoresis will be addressed elsewhere.

The result (4.26) applies to the electrophoresis of particles toward a constant potential electrode, a situation encountered in electro-deposition of colloids at metallic surfaces. Because the boundary is at uniform potential, there is no tangent electric field at the boundary and hence no electro-osmotic flow in this problem; the particle velocity is independent of ζ_w in this case. Our result shows that charged particles can be forced toward surfaces by the electrophoresis without significant hindrance (say, 25 %) until the surface-to-surface separation is about 0.4 or less of the particle radius, whereas such hindrances to diffusional fluxes occur when the separation is as large as 5 times the particle radius (see figure 3). Morrison & Stukel (1970) also considered this electrophoretic motion and solved the electrostatic and hydrodynamic problems using bipolar coordinates with numerical evaluation of the coefficients appearing in the general solution. Because their numerical results are only presented in a small graph, a clear comparison with our analytical results cannot be made.

This research was supported by the National Science Foundation and the Westvaco Corporation.

REFERENCES

ADAMSON, A. W. 1982 *Physical Chemistry of Surfaces*. Wiley-Interscience.

ANDERSON, J. L., LOWELL, M. E. & PRIEVE, D. C. 1982 Motion of a particle generated by chemical gradients, Part 1. Non-electrolytes. *J. Fluid Mech.* **117**, 107.

ANDERSON, J. L. 1983 Movement of a semipermeable vesicle through an osmotic gradient. *Phys. Fluids* **26**, 2871.

ANDERSON, J. L. 1985 Effect of nonuniform zeta potential on particle movement in electric fields. *J. Coll. Interface Sci.* (to appear).

BRENNER, J. 1961 The slow motion of a sphere through a viscous fluid towards a plane surface. *Chem. Engng Sci.* **16**, 242.

BRENNER, H. 1964*a* The Stokes resistance of a slightly deformed sphere. *Chem. Engng Sci.* **19**, 519.

BRENNER, H. 1964*b* The Stokes resistance of an arbitrary particle – IV. Arbitrary fields of flow. *Chem. Engng Sci.* **19**, 703.

DEBLOIS, R. W. & BEAN, C. P. 1970 Counting and sizing of submicron particles by the resistive pulse technique. *Rev. Sci. Instrum.* **41**, 909.

DUKHIN, S. S. & DERJAGUIN, B. V. 1974 Electrokinetic phenomena. In *Surface and Coll. Science* (ed. E. Matijevic), vol. 7. Wiley.

HAPPEL, J. & BRENNER, H. 1973 *Low Reynolds Number Hydrodynamics*. Noordhoff.

HAPPEL, J. & BYRNE, B. J. 1954 Motion of a sphere and fluid in a cylindrical tube. *Ind. Engng Chem.* **46**, 1181.

HUNTER, R. J. 1981 *Zeta Potential in Colloid Science*. Academic.

LEVINE, S., MINGINS, J. & BELL, G. M. 1967 The discrete-ion effect in ionic double-layer theory. *J. Electroanal. Chem.* **13**, 280.

MORRISON, F. A. 1970 Electrophoresis of a particle of arbitrary shape. *J. Coll. Interface Sci.* **34**, 210.

MORRISON, F. A. & STUKEL, J. J. 1970 Electrophoresis of an insulating sphere normal to a conducting plane. *J. Coll. Interface Sci.* **33**, 88.

NEWMAN, J. S. 1973 *Electrochemical Systems*. Prentice-Hall.

O'BRIEN, R. W. 1983 The solution of the electrokinetic equations for colloidal particles with thin double layers. *J. Coll. Interface Sci.* **92**, 204.

O'BRIEN, R. W. & HUNTER, R. J. 1981 The electrophoretic mobility of large colloidal particles. *Can. J. Chem.* **59**, 1878.

O'BRIEN, R. W. & WHITE, L. R. 1978 Electrophoretic mobility of a spherical colloidal particle. *J. Chem. Soc. Faraday II* **74**, 1607.

PRIEVE, D. C., ANDERSON, J. L., EBEL, J. P. & LOWELL, M. E. 1984 Motion of a particle generated by chemical gradients, Part 2. Electrolytes. *J. Fluid Mech.* **148**, 247.

SONSHINE, R. M., COX, R. G. & BRENNER, H. 1966 The Stokes translation of a particle of arbitrary shape along the axis of a circular cylinder. *Appl. Sci. Res.* **16**, 273.

YOUNG, N. O., GOLDSTEIN, J. S. & BLOCK, M. J. 1959 The motion of bubbles in a vertical temperature gradient. *J. Fluid Mech.* **6**, 350.